Geophysical Research Letters

RESEARCH LETTER
10.1029/2023GL103990

Unrestricted Solar Energetic Particle Access to the Moon While Within the Terrestrial Magnetotail

Lucas Liuzzo[1], Andrew R. Poppe[1], Christina O. Lee[1], Shaosui Xu[1], and Vassilis Angelopoulos[2]

[1]Space Sciences Laboratory, University of California, Berkeley, Berkeley, CA, USA, [2]Department of Earth and Space Sciences, University of California, Los Angeles, Los Angeles, CA, USA

Key Points:

- The two Acceleration, Reconnection, Turbulence, and Electrodynamics of the Moon's Interaction with the Sun probes observe Solar Energetic Particle (SEP) events at the Moon when located deep within the terrestrial magnetotail
- SEPs enter the magnetotail far downstream beyond the lunar orbit, along open field lines that are connected on one end to Earth's polar caps
- The terrestrial magnetosphere is ineffective in shielding SEPs from accessing the lunar orbit while within the magnetotail

Supporting Information:

Supporting Information may be found in the online version of this article.

Correspondence to:

L. Liuzzo,
liuzzo@berkeley.edu

Citation:

Liuzzo, L., Poppe, A. R., Lee, C. O., Xu, S., & Angelopoulos, V. (2023). Unrestricted solar energetic particle access to the Moon while within the terrestrial magnetotail. *Geophysical Research Letters*, *50*, e2023GL103990. https://doi.org/10.1029/2023GL103990

Received 14 APR 2023
Accepted 8 JUN 2023

Abstract This study presents observations of Solar Energetic Particle (SEP) protons that have penetrated Earth's magnetotail to reach the lunar environment. We apply data from Wind as an upstream monitor and compare to observations from THEMIS-ARTEMIS within the tail to show clear signatures of SEPs at the Moon during two events. Combining modeling and data analysis, we show that SEPs above energies of ∼25 keV gain access to the Moon's position deep within the magnetotail through field lines that are open on one end to the solar wind. These results contradict previous studies that have suggested that the magnetotail is effective in shielding the Moon from SEPs with energies up to 1 GeV. Instead, we highlight that Earth's magnetosphere provides poor protection to the Moon from SEPs, which irradiate the lunar surface even within the tail. Our results have important implications regarding the safety of astronauts during upcoming lunar missions.

Plain Language Summary During two thirds of its orbit, the Moon is located outside of Earth's magnetosphere. At these locations, the lunar surface is exposed to a variety of charged particles including (low-energy) solar wind plasma and (high-energy) Solar Energetic Particles (SEPs), the latter of which are responsible for weathering and chemically altering the lunar surface. For the remaining one third of its orbit, the Moon is located within Earth's magnetosphere. Previous studies have suggested that the ambient magnetic field within this cavity shields the Moon from the highly energetic SEPs. However, we report clear observations by NASA's THEMIS-ARTEMIS mission of these potentially hazardous charged particles when the Moon was embedded deep within Earth's magnetosphere. We also apply computer simulations to illustrate that Earth's magnetic tail is porous, allowing SEPs to efficiently leak into the terrestrial magnetosphere. Our findings are therefore highly relevant for the safety of astronauts during the upcoming missions to explore the lunar environment.

1. Introduction

Solar Energetic Particles (SEPs) are ions and electrons that are transported outward throughout the heliosphere, exceeding energies of $E \gtrsim 10$ keV (e.g., Hultqvist et al., 1999; Lin, 1987; Reames, 1999). As SEPs propagate through the heliosphere, they have a variety of impacts on planetary bodies (e.g., Leblanc et al., 2003; Lee et al., 2018; Plainaki et al., 2016). At the Moon, long exposures to these SEPs weather and chemically alter the lunar surface (e.g., Crites et al., 2013; Delitsky et al., 2017; Poppe, Farrell, & Halekas, 2018), stimulating organic synthesis of ice-rich regions located, for example, within the permanently shadowed cold traps of the lunar poles (Lucey, 2000). Over shorter timescales, particle precipitation during high-flux SEP events charges the lunar nightside surface to potentials reaching nearly −5 kV (Halekas et al., 2007, 2009). While electrostatic discharge associated with such large negative potentials represents a severe hazard for any type of lunar exploration, direct irradiation of astronauts by SEPs during lunar missions represents a clear hazard to the health and safety of the crew (e.g., Atri et al., 2022; English et al., 1973; Zeitlin et al., 2018).

The Moon (radius R_L = 1,737.4 km) orbits Earth at a distance of approximately $60R_E$ (radius of Earth R_E = 6,371 km). For nearly two thirds of its orbit, the Moon is located outside of Earth's magnetosphere, so its dayside surface is unprotected from continuous influx of solar wind and energetic particles during SEP events. While particles with gyroradii below a lunar radius are shielded from one hemisphere of the surface by the solid body of the Moon (depending on the IMF orientation and the Moon's connection to the particle source; see e.g., Fatemi et al., 2012; Lin, 1968; Liuzzo et al., 2021; Van Allen & Ness, 1969), spacecraft observations show that particles at energies $E \gtrsim 100$ keV (i.e., SEPs and Galactic Cosmic Rays; GCRs) precipitate nearly unimpeded

due to their much larger gyroradii ($\gg R_L$; see X. Xu et al., 2017; Z. Xu et al., 2020). During the remaining one third of its orbit, the Moon is located within the terrestrial magnetosphere. Here, the Moon is exposed to multiple plasma environments, including the shocked plasma within the magnetosheath, the terrestrial plasma sheet, and the tenuous plasma of the lobes (e.g., Liuzzo, Poppe, & Halekas, 2022).

As the Moon travels through Earth's magnetotail, the local field may likewise limit energetic particle access to the lunar surface (e.g., Størmer, 1955). Such shielding could curb the role that these particles have in processing the surface, limiting the hazards associated with their precipitation whenever the Moon is embedded within the tail. To estimate the energies below which particles could be prevented from reaching the Moon while within the tail, Winglee and Harnett (2007) applied a multi-fluid model of Earth's magnetosphere to calculate the magnetic field strength along the lunar orbit. They suggested that particles below energies of $E \approx 1$ GeV could be shielded from the lunar surface, depending on the orientation of the IMF. Separately, Harnett (2010) applied this model to constrain energetic particle access to the Moon within the tail, for times when Earth's magnetosphere is perturbed during, for example, an interplanetary coronal mass ejection (ICME). Under these storm-time conditions, Harnett (2010) stated that particles below 35 MeV are prevented from reaching the Moon. More recently, Jordan et al. (2022) suggested that the gyroradius of a charged particle must exceed the radius of the terrestrial magnetotail at the Moon's orbital position in order to precipitate onto the lunar surface when in the tail, arguing that particles with smaller gyroradii would be significantly deflected and unable to reach the Moon (see also Winglee & Harnett, 2007). Hence, they argued that protons below 100 MeV, and electrons below 1 GeV, are prevented from reaching the lunar environment when embedded within the magnetotail.

However, multiple observational and modeling studies contradict these results, instead suggesting that particles with much lower energies reach the Moon when in the tail. Using data from the Cosmic Ray Telescope for the Effects of Radiation (CRaTER) instrument onboard the Lunar Reconnaissance Orbiter, Case et al. (2010) reported that the magnetotail is ineffective at shielding particles above 14 MeV (the lowest energy measured by CRaTER). These authors found that above this energy, the instrument observed a reduction in the particle flux by less than 2% when transiting through the magnetotail. Similarly, Chandrayaan-1 and Chang'E-1 measurements suggest no significant decrease of particles at energies above ∼10 MeV within the tail (Jie & Gang, 2013; Koleva et al., 2010). Finally, Huang et al. (2009) modeled the trajectories of test-particles at energies 1 MeV $\leq E \leq$ 100 MeV to constrain their access to the Moon as it passes through the tail, finding that these particles are *unaffected* by the magnetosphere.

Only a single study by X. Xu et al. (2017) has investigated the ability of $E \lesssim 1$ MeV SEP protons to penetrate the terrestrial magnetotail and reach the lunar orbit. They applied measurements from the Solid State Telescopes (SSTs) onboard the *Acceleration, Reconnection, Turbulence, and Electrodynamics of the Moon's Interaction with the Sun* (ARTEMIS; Angelopoulos, 2011) probes, focusing on SEP events that occurred while ARTEMIS (and hence, the Moon) was within the tail. For example, one event studied by X. Xu et al. (2017) occurred on 23–24 June 2013, during which the SSTs onboard NASA's Wind spacecraft (Harten & Clark, 1995) observed an enhanced SEP ion population upstream of Earth at energies 100 keV $\leq E \leq$ 7 MeV. Similarly, ARTEMIS observed enhanced fluxes during this time, but also detected signatures of intermittent hot magnetotail plasma below $E \lesssim 100$ keV. X. Xu et al. (2017) argued that these measurements in the low-energy channels contaminated the SST observations with background signals of secondary particles (even those channels extending beyond energies of 100 keV) and stated that the fluxes observed by ARTEMIS during this event were not associated with SEPs. Based on their findings, these authors concluded that the magnetosphere shields all SEPs at energies below $E \lesssim 4$ MeV from reaching the Moon's environment when located within the tail. However, this contradicts the modeling results of Huang et al. (2009) which suggest that 1 MeV protons *can* reach the lunar orbit, even within the tail.

To understand effects including space weathering of the lunar surface (e.g., Crites et al., 2013; Jordan et al., 2023; Poppe, Farrell, & Halekas, 2018) and to appreciate possible hazards to astronaut safety associated with radiation from these high-energy particles, it is critical to determine whether SEPs can penetrate the magnetotail fields to reach the lunar environment and to constrain the energies at which SEPs access the lunar surface. Here, we present case studies of two events observed by ARTEMIS that clearly illustrate the Moon is fully exposed to upstream SEP protons, even while located deep within in the terrestrial magnetotail. We combine magnetohydrodynamic and test-particle simulations to show that SEPs access the terrestrial magnetotail at distances of several hundred R_E downtail along open field lines that are connected on one end to Earth's polar caps.

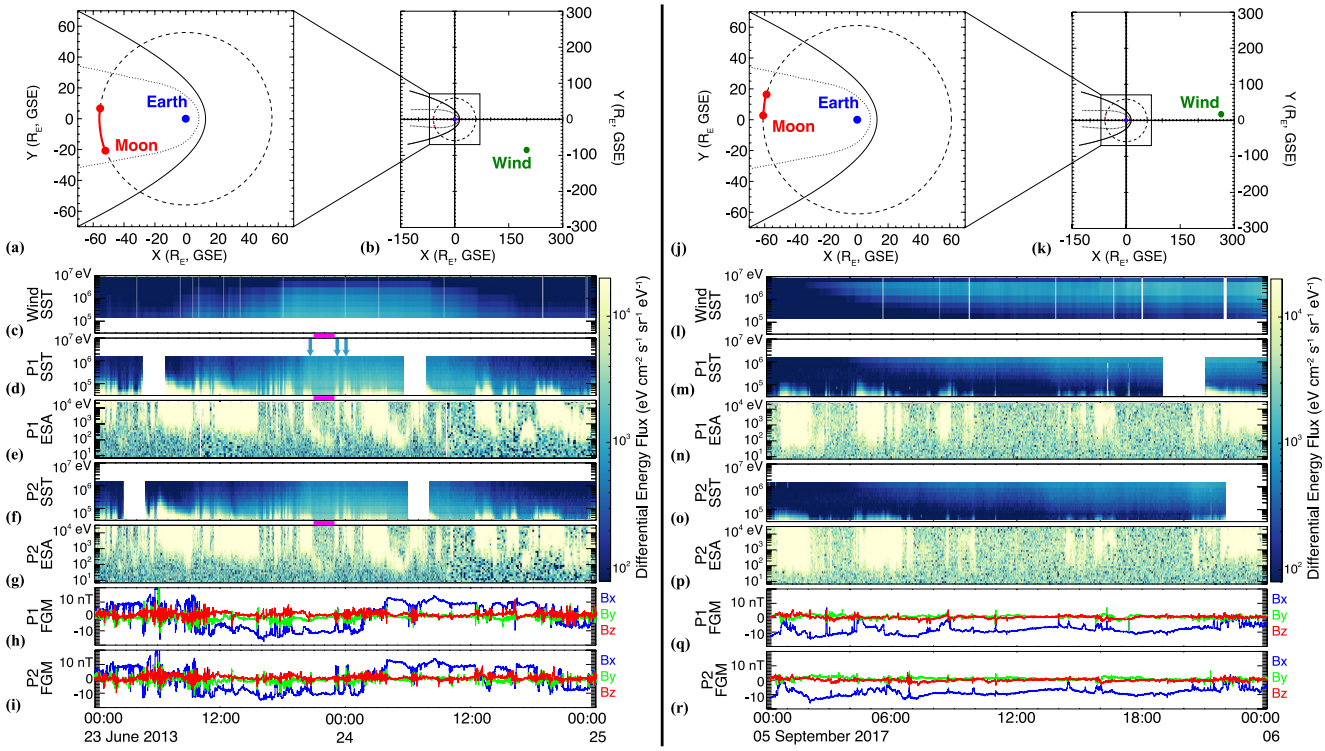

Figure 1. SEP events during (a–i) 23–25 June 2013 and (j–r) 05 September 2017. Panels (a, j) illustrate the position of the Moon and Earth; panels (b, k) show the position of Wind. Differential energy fluxes from SST open channels are shown from (c, l) Wind, (d, m) P1, and (f, o) P2; ESA differential energy fluxes are shown from (e, n) P1 and (g, p) P2. Two-hour data gaps correspond to P1 and P2 closest approaches, when SST attenuators are activated to limit moonshine. ARTEMIS (h–i) P1 and (q–r) P2 magnetic field measurements are shown in the Geocentric Solar Ecliptic (GSE) coordinate system.

2. The Wind and ARTEMIS Missions

Onboard Wind is a suite of instruments to study the plasma environment near 1 AU, including the SST (Lin et al., 1995) which measures ions from 100 keV $\lesssim E \lesssim$ 7 MeV and electrons from 25 keV $\lesssim E \lesssim$ 500 keV. Located approximately $200R_E$ upstream of Earth at the Sun-Earth L1 point since 2004, Wind's observations are indicative of the "pristine" plasma environment before being perturbed by the terrestrial magnetosphere. The two ARTEMIS probes, originally part of the *Time History of Events and Macroscale Interactions during Substorms* (THEMIS; Angelopoulos, 2008) mission, have been in lunar orbit since 2011. Each probe, P1 and P2, is equipped with an identical instrument suite, including SSTs that are nearly identical to those on Wind (cf. Angelopoulos, 2008; Angelopoulos, 2011; Lin et al., 1995), measuring particles above $E \geq 25$ keV and up to $E \lesssim 5$ MeV (ions) or $E \lesssim 600$ keV (electrons). The SSTs consist of two sensors, each comprised of a pair of double-ended telescopes with a stacked triplet of silicon detectors. In the absence of penetrating radiation, one end of the telescopes measures ions while the other measures electrons. In addition, the ARTEMIS probes have an electrostatic analyzer (ESA; McFadden et al., 2008) measuring ions and electrons for energies 6 eV $\lesssim E \lesssim$ 30 keV, and a fluxgate magnetometer (FGM; Auster et al., 2008).

3. Access of Solar Energetic Particles to the Terrestrial Magnetotail

3.1. Observations of SEPs Within the Tail

Figures 1a–1i display Wind and ARTEMIS observations from 23 to 24 June 2013, the same SEP event presented by X. Xu et al. (2017). This event was likely associated with a fast CME that erupted on 21 June from solar active region (AR) 11777, which produced an observed coronal shock wave and associated widespread SEPs that were observed by multiple spacecraft throughout the inner heliosphere (see Frassati et al., 2022; Winslow et al., 2015). Panels 1a and 1b show the location of the Moon and the Wind spacecraft, respectively, during this event, illustrating the position of ARTEMIS well within the terrestrial magnetotail (see also the orientation of the magnetic field

with its strong Earthward/anti-Earthward component, provided in panels 1h–1i). Energetic ion measurements from the Wind, P1, and P2 SSTs are included in panels 1c, 1d, and 1f, respectively. In addition, ARTEMIS ESA ion measurements are shown in panels 1e and 1g.

The ICME associated with this June event did not directly impact Earth; see, for example, the Richardson and Cane ICME list (Richardson & Cane, 2010) or the Kasper and Stevens shock list. Nevertheless, Figure 1c shows that Wind clearly observed a broad signature of "energetic storm particles" (SEPs accelerated locally by a passing ICME; see Cohen, 2006) beginning near 12:00 on 23 June and lasting ∼24 hr, with all but the highest SST energy channel displaying an enhanced differential energy flux. Panels 1d and 1f illustrate that a nearly identical enhancement was observed by the ARTEMIS SSTs at energies 100 keV $\lesssim E \lesssim$ 1 MeV during this time. This enhancement even extends to the lowest SST energy channel of ∼25 keV. However, below $E \lesssim$ 100 keV, this signature is overlain by intermittent injections of hot plasma associated with the magnetotail plasma sheet (e.g., Artemyev et al., 2017), as also detected by the ARTEMIS ESAs at energies as low as ∼500 eV (see panels 1e and 1g). Even during these times with the probes located within the sheet, the signature of $E >$ 100 keV particles in the ARTEMIS observations is evident. Interestingly, panels 1d and 1f illustrate that the probes detected SEPs while in both magnetotail lobes (see panels 1h and 1i). Indeed, Wind observed a nearly isotropic SEP pitch angle distribution, suggesting that both lobes—open to oppositely-oriented IMF field lines—were suffused with SEPs during this event. The similarity between the Wind and ARTEMIS SST observations at energies above 100 keV suggest that Earth's magnetotail plays only a limited role in preventing SEP access to the Moon.

Figures 1j–1r include Wind and ARTEMIS observations during a second SEP event occurring on 05 September 2017. These particles were likely associated with an M5.5 solar flare that erupted from AR 12673 at 20:15 on 04 September. Again, the position of the Moon (panel 1j), the low-energy ion differential energy fluxes observed by ARTEMIS (panels 1n and 1p), and the nearly constant, tailward magnetic field ($B_x < 0$; panels 1q–1r) indicate that the Moon was located deep within the southern lobe of the terrestrial magnetotail during this event. And yet, like the observations during the June 2013 SEP event, the Wind $E >$ 100 keV ion differential energy flux (panel 1l) is nearly identical to the ARTEMIS signatures (panels 1m and 1o). Notably, the SST energy fluxes are dispersive in that they demonstrate a clear dependence on energy: the highest-energy protons (with highest velocities) arrive to the detectors first, followed by protons at successively lower energies. This dispersion is consistent with the signature of SEPs when magnetically connected to a solar flare (e.g., Reames, 2013), and the dispersive structure is preserved even within the magnetotail. The Wind and ARTEMIS observations during these two separate SEP events are nearly identical, demonstrating that the magnetotail is *unable* to effectively shield SEP ions above $E \approx$ 100 keV from accessing the lunar environment, contradicting findings from previous studies (e.g., Harnett, 2010; Jordan et al., 2022; Winglee & Harnett, 2007; X. Xu et al., 2017).

To further elucidate the similarity between these signatures, Figure 2a compares the $E >$ 100 keV ion spectrum observed by Wind (blue) and ARTEMIS P1 (green) during the June 2013 SEP event (see Figures S1 and S2 in Supporting Information S1 for additional comparisons). These spectra in panel 2a are averaged over a two-hour period from 20:50–22:50 on the 23rd (see pink bars at the bottom of panels 1c, 1d, and 1f, and 2b), while P1 was in the southern lobe of the terrestrial magnetotail to ensure that the SST measurements were not contaminated by any hot magnetotail plasma. The two spectra in Figure 2a are nearly identical (but differ by up to a factor of ∼1.1 due to, e.g., different instrument calibrations), despite the spacecraft being located within two vastly different regions (Wind upstream of Earth in the solar wind, and ARTEMIS deep within Earth's magnetotail). Panel 2a therefore confirms that the enhanced differential energy fluxes detected by ARTEMIS are SEPs that penetrated the magnetosphere and were detected, nearly unaltered, deep within the magnetotail.

Furthermore, Figure 2b shows the Wind (blue) and ARTEMIS P1 (green) differential ion energy fluxes of 1 MeV protons for this SEP event. Near 18:00 on the 23rd, the 1 MeV Wind proton differential energy flux sharply increased by a factor of 2 in ∼10 min (labeled "onset"), reaching a value of 600 eV cm^{-2} s^{-1} sr^{-1} eV^{-1}. This flux was sustained for ∼1 hr, before further increasing to a peak value of ∼800 eV cm^{-2} s^{-1} sr^{-1} eV^{-1} near 19:30. Over the next 12 hr, the differential energy flux gradually decreased, until a rapid subsidence in the 1 MeV differential energy flux at 08:00 on 24 June. Panel 2b illustrates that P1 observed nearly identical features that were time-shifted compared to the Wind observations. To further highlight this delay, the yellow curve in Figure 2b again shows the Wind observations, but now shifted by 2 hours to coincide with the observed ARTEMIS 1 MeV SEP enhancement. With this shift, multiple features of the Wind and ARTEMIS data occur at nearly identical times, including the 1 MeV differential energy flux onset, the ∼12-hr decrease, and the rapid subsidence where fluxes return to background (see also Figure 1).

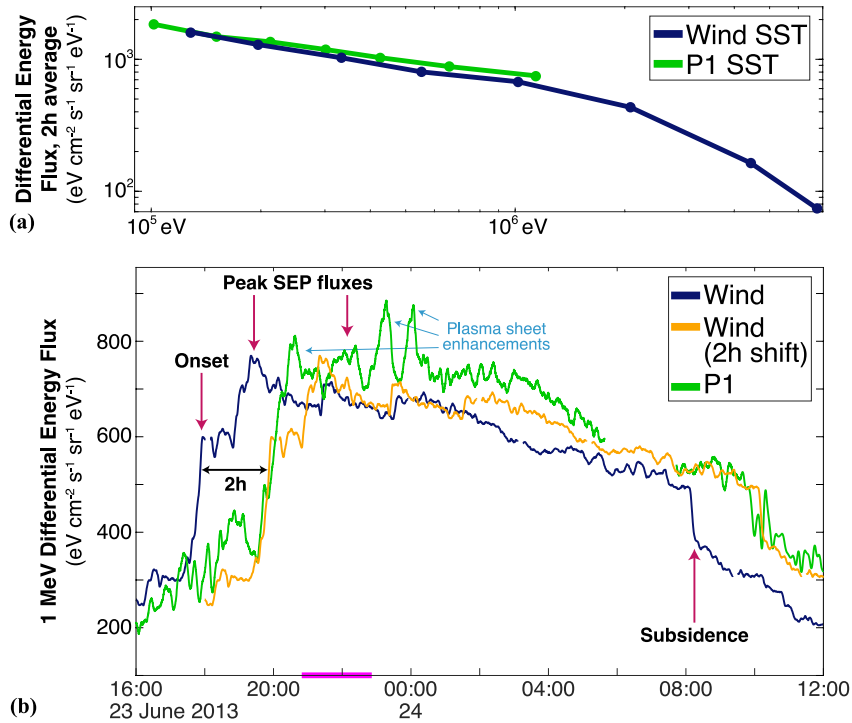

Figure 2. Differential ion energy flux during the June 2013 SEP event observed by Wind (blue) and ARTEMIS P1 (green). Panel (a) displays the $E > 100$ keV ion spectra averaged over a two-hour window from 20:50–22:50 on the 23rd, whereas panel (b) displays a five-minute running average of 1 MeV ion differential energy fluxes from 16:00 on the 23rd through 12:00 on the 24th. The yellow line in panel (b) shows the Wind observations shifted by 2 hours. The pink bar indicates the time over which the fluxes in panel (a) are averaged.

However, certain features of the ARTEMIS differential energy flux are not present in the time-shifted Wind observations. The most obvious differences are three narrow spikes, visible near 21:00 on the 23rd and 00:00 on the 24th. Here, the P1 1 MeV differential flux reached nearly 900 eV cm^{-2} s^{-1} sr^{-1} eV^{-1} (light blue arrows in Figure 2b): ∼1.2 times above the maximum observed by Wind, which did not observe qualitatively similar features during these periods. These spikes are associated with the magnetotail plasma sheet (see light blue arrows above panels 1d–1e), where P1 detected an enhanced ion flux extending down to energies of ∼1 keV. A second discrepancy regards the timing of the peak SEP differential energy flux. Although the ARTEMIS SEP 1 MeV onset occurred almost exactly 2 hr after Wind, the peak P1 flux occurred ∼2.5 hr after the Wind peak. However, the maximum amplitude and structures of the peaks observed by both spacecraft closely match.

The agreement between the ARTEMIS and time-shifted Wind observations (Figure 2b) suggests that these SEPs required ∼2 additional hours to reach the Moon, consistent with the local generation of energetic storm particles as an ICME passed nearby. Using the WSA-ENLIL + Cone model for this June 2013 event available at NASA's Community Coordinated Modeling Center (CCMC; see kauai.ccmc.gsfc.nasa.gov/DONKI/view/WSA-ENLIL/2586/1), we estimate a velocity of 800 km/s as this ICME passed near Earth. Hence, this ICME traveled ∼900R_E in the 2-hr offset between the Wind and ARTEMIS observations. Since Wind was located 200R_E upstream, this suggests these SEP entered the magnetosphere ∼640R_E beyond the Moon's orbit. Note that since these SEPs were generated locally (i.e., not at the Sun) and travel more than an order of magnitude faster than the ICME, any path difference between the protons detected by Wind and ARTEMIS plays only a minor role in any temporal offset between the observations.

Notably, despite the suggestions of X. Xu et al. (2017), the SST signatures during this event were not caused by high-energy particles contaminating the sensors. While penetration of highly energetic ions ($E \gtrsim 10$ MeV) may contaminate the SSTs, additional spacecraft upstream of Earth (e.g., the Advanced Composition Explorer and the Solar and Heliospheric Observatory) with separate instrumentation show nearly identical enhancements. Likewise, while high energy electrons may also contaminate the SST detectors, the Wind and ARTEMIS $E \gtrsim 400$ keV

electron fluxes were not enhanced, so penetrating electrons can be ruled out. Instead, the SST observations indicate SEP entry into Earth's magnetotail.

Figure S2 in Supporting Information S1 presents a comparison between the Wind and ARTEMIS spectra for the September SEP event, in the same style as Figure 2. Again, the spectra of the Wind and ARTEMIS differential energy fluxes, respectively, are in close agreement, despite the position of P1 and P2 deep within the magnetotail. Note that unlike for the June event, there is no appreciable time-shift between the Wind and ARTEMIS observations, consistent with the signature of SEPs generated by a solar flare.

3.2. Modeling SEP Access to the Tail

To better understand SEP dynamics and to shed light on their access to the Moon, we traced test particle trajectories as they travel through the terrestrial magnetosphere. We apply the Open Geospace General Circulation Model (OpenGGCM; e.g., Fuller-Rowell et al., 1996; Raeder et al., 2017), available at the CCMC, to calculate global plasma and electromagnetic field quantities. For this analysis, we focus on the June 2013 SEP event; results from the September 2017 event are shown in Figure S3 in Supporting Information S1. OpenGGCM is driven with the conditions observed upstream by Wind for the 24-hr period from 12:00 on 23 June 2013 through 12:00 on 24 June; that is, the center interval shown in Figure 1. In GSE coordinates, the OpenGGCM spatial domain extends from $-350R_E \leq x \leq +33R_E$ (along the Sun-Earth line), and from $-96R_E \leq y, z \leq +96R_E$. Thus, this domain includes a large portion of the Moon's orbit, including its magnetotail passage. Three-dimensional data cubes of the plasma density, plasma velocity, and electromagnetic fields are output every 240 s. Comparison of OpenGGCM with the ARTEMIS P1 and P2 observations show moderate agreement, sufficient to proceed with test-particle tracing.

Following the approach of Poppe et al. (2016), protons with mass 1 amu are initialized at the Moon within the OpenGGCM electromagnetic field output at a specific time, position, energy, and pitch angle corresponding to the observed SEPs (see Figure 1). Trajectories are then integrated backwards in time using a Runge-Kutta-4 algorithm to solve the Lorentz force law, thereby allowing for an assessment of the particles' behavior leading up to their detection by ARTEMIS. Each particle is followed until it strikes one of the outer simulation boundaries (no particles reached OpenGGCM's inner boundary located at $\sim 3R_E$). This backtracking method is much more computationally efficient than an approach where particles would be initialized upstream of Earth and traced forward in time (see also, e.g., Poppe, Fatemi, & Khurana, 2018; Liuzzo, Poppe, Addison, et al., 2022; Liuzzo et al., 2019a, 2019b, 2020). Figure 3 shows a representative set of test-particle trajectories in the GSE (3a–3c) x-y and (3d–3f) x-z planes for select energies (25, 50, 150, 350, 750, and 1,000 keV) over-plotted on the OpenGGCM results for the magnetic field magnitude (3a, 3d), plasma bulk velocity (3b, 3e), and number density (3c, 3f) during the June 2013 SEP event. These particles were initialized at midnight on 24 June with initial pitch angles of 180°, such that they traveled toward Earth when integrating backwards in time.

When considered going forwards in time, these results illustrate that the SEP protons travel large distances within the terrestrial magnetotail before their detection by ARTEMIS. The two lowest-energy test particles at 25 and 50 keV (blue and green in Figure 3) entered the distant magnetotail near $x \approx -275R_E$ and $x \approx -300R_E$, respectively. The "elbow" visible in each of their trajectories denotes the point at which they crossed the magnetopause (as also confirmed by inspection of the local electromagnetic fields along each particle's trajectory, which is omitted from the figure for clarity). As SEPs approach the Moon from downtail, some impact the lunar nightside, as is consistent with observations from Explorer 35 of "lunar shadowing" of ions and electrons, whereby the surface of the Moon prevented detection of energetic particles during cis-lunar transits of the spacecraft (e.g., Lin, 1968; Van Allen, 1970; Van Allen & Ness, 1969). However, the 25 and 50 keV particles illustrated in Figure 3 continue traveling toward upstream, initially passing by the Moon before eventually encountering the enhanced magnetic fields close to Earth (near $x \approx -5R_E$). Although beyond the focus of this study, penetration of SEPs to these magnetospheric locations is consistent with preliminary analysis of the SSTs on the three inner THEMIS probes during this event, which also show signatures of enhanced energetic proton energy fluxes. The enhanced fields near the Earth cause the 25 and 50 keV test particles displayed in Figure 3 to mirror, where they begin traveling tailwards before impacting the lunar dayside or (in the case of Figure 1) being detected by ARTEMIS.

Higher-energy backtracked particles (150 keV $\leq E \leq$ 1 MeV; see Figure 3) encounter the OpenGGCM boundary before exiting the tail. While the behavior of the 25 and 50 keV ions implies that, in forward time, these

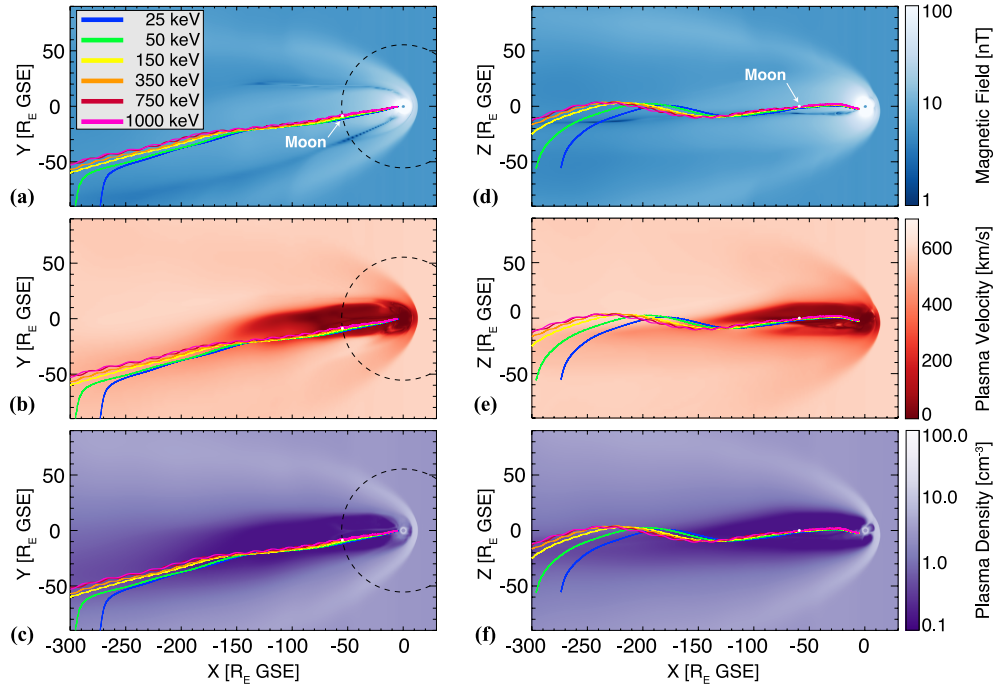

Figure 3. Proton trajectories at select energies from 25 keV ≤ E ≤ 1 MeV as they travel through the magnetosphere. Dashed curves in panels (a–c) show the lunar orbit.

higher-energy particles also enter the terrestrial magnetotail along open field lines at even greater distances (beyond $x = -350R_E$), they may instead penetrate *across* the magnetopause boundary since the magnetic field magnitude is reduced far downtail. Regardless of the process, the fact remains that SEPs enter the magnetotail far downstream at distances that are consistent with estimations based on the velocity of the ICME during this event (see Section 3.1 above) and consistent with previous studies suggesting SEP entry at locations up to 1,000 R_E downstream (e.g., Dessler, 1964; Dungey, 1965; Evans, 1972; Milan, 2004; Ness et al., 1967; Paulikas, 1974).

We simulated 25 keV ≤ E ≤ 1 MeV particles at a range of initial pitch angles and at several starting times between 12:00 on 23 June 2013 and 12:00 on the 24th, finding that a majority (~90%) demonstrated behaviors like those in Figure 3. Additional tracing confirms a similar behavior of protons entering the distant magnetotail during the 05 September 2017 event (see Figure S3 in Supporting Information S1). These tests confirm the robustness of our conclusions that SEPs access the terrestrial magnetotail far downstream along open magnetospheric field lines that have one end rooted in the terrestrial polar cap and the other end connected to the IMF.

4. Conclusions

This study has presented THEMIS-ARTEMIS observations obtained while the probes were embedded deep within Earth's magnetotail. During two SEP events, the probes observed clear signatures of energetic protons, nearly unchanged when compared to their detection upstream by Wind, indicating direct access of SEPs to the lunar orbit, even when the Moon is within the magnetotail. The open nature of the magnetic field lines suggests that the magnetosphere is ineffective in shielding particles above keV energies from reaching the Moon. This finding contradicts previous studies that have suggested that the magnetotail is effective in shielding protons from 1 to 100 MeV (e.g., Harnett, 2010; Jordan et al., 2022; Winglee & Harnett, 2007; X. Xu et al., 2017), but is consistent with observations within the tail of particles at energies $E \gtrsim 10$ MeV (Case et al., 2010).

Notably, shielding future astronauts and equipment on the lunar surface from energetic particle radiation is a key consideration of the upcoming missions to the Moon, including the crewed Artemis missions to explore the south pole. Although penetrating particles at energies greater than ~1 MeV are responsible for the most severe damage to astronauts and electronics (e.g., Cucinotta et al., 2010; Xapsos et al., 2007), our findings that SEPs at energies above 25 keV enter the magnetotail along open field lines indicate that the more damaging, higher-energy

particles likely also have nearly unrestricted access to the lunar surface. Hence, in addition to those particles at higher energies, keV-to-MeV SEPs present a clear potential hazard to future exploration of the lunar surface, even for times when the Moon is within the terrestrial magnetotail.

Data Availability Statement

THEMIS-ARTEMIS data are available at artemis.ssl.berkeley.edu or cdaweb.gsfc.nasa.gov/pub/data/themis, and Wind SST ion data can be accessed at cdaweb.gsfc.nasa.gov/pub/data/wind/3dp/3dp_sosp. OpenGGCM results are available at tinyurl.com/june2013sep and tinyurl.com/september2017sep.

Acknowledgments
The authors are supported by NASA LDAP Grant 80NSSC20K0311 and the THEMIS-ARTEMIS mission, NASA Grant NAS5-02099. C.O. Lee acknowledges support from NASA LWS Grant 80NSSC21K1325. We thank R.J. Lillis and D.E. Larson for discussions and insights into SST. We acknowledge J.P. McFadden for use of ESA data and K.-H. Glassmeier, U. Auster, and W. Baumjohann for the use of FGM data provided under the lead of the Technical University of Braunschweig and with financial support through the German Ministry for Economy and Technology and the German Center for Aviation and Space, Contract 50-OC-0302. OpenGGCM was developed by Tim Fuller-Rowell (NOAA) and Joachim Raeder (UNH), with access provided by CCMC.

References

Angelopoulos, V. (2008). The THEMIS mission. *Space Science Reviews*, *141*(1–4), 5–34. https://doi.org/10.1007/s11214-008-9336-1
Angelopoulos, V. (2011). The ARTEMIS mission. *Space Science Reviews*, *165*(1–4), 3–25. https://doi.org/10.1007/s11214-010-9687-2
Artemyev, A. V., Angelopoulos, V., Runov, A., & Vasko, I. Y. (2017). Hot ion flows in the distant magnetotail: ARTEMIS observations from lunar orbit to ∼-200 RE. *Journal of Geophysical Research: Space Physics*, *122*(10), 9898–9909. https://doi.org/10.1002/2017JA024433
Atri, D., MacArthur, C., Devata, S., Herbst, K., Gakis, D., Mathur, S., et al. (2022). Crewed missions to Mars: Modeling the impact of astrophysical charged particles on astronauts and their health. arXiv. Retrieved from http://arxiv.org/abs/2208.00892
Auster, H. U., Glassmeier, K. H., Magnes, W., Aydogar, O., Baumjohann, W., Constantinescu, D., et al. (2008). The THEMIS fluxgate magnetometer. *Space Science Reviews*, *141*(1–4), 235–264. https://doi.org/10.1007/s11214-008-9365-9
Case, A. W., Spence, H. E., Golightly, M. J., Kasper, J. C., Blake, J. B., Mazur, J. E., et al. (2010). GCR access to the Moon as measured by the CRaTER instrument on LRO. *Geophysical Research Letters*, *37*(19), 1–5. https://doi.org/10.1029/2010GL045118
Cohen, C. (2006). Observations of energetic storm particles: An overview. In N. Gopalswamy, R. Mewaldt, & J. Torsti (Eds.), *Solar eruptions and energetic particles*. John Wiley & Sons, Inc. https://doi.org/10.1029/165GM26
Crites, S. T., Lucey, P. G., & Lawrence, D. J. (2013). Proton flux and radiation dose from galactic cosmic rays in the lunar regolith and implications for organic synthesis at the poles of the Moon and Mercury. *Icarus*, *226*(2), 1192–1200. https://doi.org/10.1016/j.icarus.2013.08.003
Cucinotta, F. A., Hu, S., Schwadron, N. A., Kozarev, K., Townsend, L. W., & Kim, M.-H. Y. (2010). Space radiation risk limits and Earth-Moon-Mars environmental models. *Space Weather*, *8*(12), S00E09. https://doi.org/10.1029/2010SW000572
Delitsky, M. L., Paige, D. A., Siegler, M. A., Harju, E. R., Schriver, D., Johnson, R. E., & Travnicek, P. (2017). Ices on Mercury: Chemistry of volatiles in permanently cold areas of Mercury's North Polar Region. *Icarus*, *281*, 19–31. https://doi.org/10.1016/j.icarus.2016.08.006
Dessler, A. J. (1964). Length of magnetospheric tail. *Journal of Geophysical Research*, *69*(19), 3913–3918. https://doi.org/10.1029/JZ069i019p03913
Dungey, J. W. (1965). The length of the magnetospheric tail. *Journal of Geophysical Research*, *70*(7), 1753. https://doi.org/10.1029/JZ070i007p01753
English, R. A., Benson, R. E., Bailey, J. V., & Barnes, C. M. (1973). Apollo experience report: Protection against radiation. NASA Technical Report(NASA-TN-D-7080).
Evans, L. C. (1972). *Magnetospheric access of solar particles and the configuration of the distant geomagnetic field*. Doctoral dissertation, California Institute of Technology. https://doi.org/10.7907/vzsp-g414
Fatemi, S., Holmstrm, M., & Futaana, Y. (2012). The effects of lunar surface plasma absorption and solar wind temperature anisotropies on the solar wind proton velocity space distributions in the low-altitude lunar plasma wake. *Journal of Geophysical Research*, *117*(10), 1–13. https://doi.org/10.1029/2011JA017353
Frassati, F., Laurenza, M., Bemporad, A., West, M. J., Mancuso, S., Susino, R., et al. (2022). Acceleration of solar energetic particles through CME-driven shock and streamer interaction. *The Astrophysical Journal*, *926*(2), 227. https://doi.org/10.3847/1538-4357/ac460e
Fuller-Rowell, T., Rees, D., Quegan, S., Moffett, R., Codrescu, M., & Millward, G. (1996). A coupled thermosphere-ionosphere model (CTIM). STEP report scientific committee on solar terrestrial physics (SCOSTEP). *NOAA/NGDC*, *239*(4).
Halekas, J. S., Delory, G. T., Brain, D. A., Lin, R. P., Fillingim, M. O., Lee, C. O., et al. (2007). Extreme lunar surface charging during solar energetic particle events. *Geophysical Research Letters*, *34*(2), 1–5. https://doi.org/10.1029/2006GL028517
Halekas, J. S., Delory, G. T., Lin, R. P., Stubbs, T. J., & Farrell, W. M. (2009). Lunar surface charging during solar energetic particle events: Measurement and prediction. *Journal of Geophysical Research*, *114*(5), 1–16. https://doi.org/10.1029/2009JA014113
Harnett, E. M. (2010). Deflection and enhancement of solar energy particle flux at the Moon by structures within the terrestrial magnetosphere. *Journal of Geophysical Research*, *115*(A1), A01210. https://doi.org/10.1029/2009JA014209
Harten, R., & Clark, K. (1995). The design features of the GGS wind and polar spacecraft. *Space Science Reviews*, *71*(1–4), 23–40. https://doi.org/10.1007/BF00751324
Huang, C.-L., Spence, H. E., & Kress, B. T. (2009). Assessing access of galactic cosmic rays at Moon's orbit. *Geophysical Research Letters*, *36*(9), L09109. https://doi.org/10.1029/2009GL037916
Hultqvist, B., Øieroset, M., Paschmann, G., & Treumann, R. A. (1999). Source and loss processes in the inner magnetosphere. *Magnetospheric Plasma Sources and Losses: Final Report of the ISSI Study Project on Source and Loss Processes*, 137–206.
Jie, W., & Gang, Q. (2013). Study of magnetospheric shielding effect with energetic particles data from Chang'E-1. *Chinese Journal of Space Science*, *33*(5), 532–539. https://doi.org/10.11728/cjss2013.05.532
Jordan, A. P., Case, A. W., Wilson, J. K., & Huang, C.-L. (2022). Evidence that Earth's magnetotail affects dielectric breakdown weathering on the Moon. *Icarus*, *383*, 115011. https://doi.org/10.1016/j.icarus.2022.115011
Jordan, A. P., Wilson, J. K., & Spence, H. E. (2023). Energetic charged particle dose rates in water ice on the Moon. *Icarus*, *395*, 115477. https://doi.org/10.1016/j.icarus.2023.115477
Koleva, R., Tomov, B., Dachev, T., Matviichuk, Y., & Dimitrov, P. (2010). Effects of the terrestrial magnetosphere on radiation hazard on Moon missions. In *Sixth scientific conference with international participation SES*. Retrieved from https://www.researchgate.net/profile/Rositza-Koleva/publication/289664975_Moon_radiation_environment_in_the_vicinity_of_earth_magnetosphere/links/5aa7ed640f7e9b0ea3079719/Moon-radiation-environment-in-the-vicinity-of-earth-magnetosphere.pdf
Leblanc, F., Luhmann, J., Johnson, R., & Liu, M. (2003). Solar energetic particle event at Mercury. *Planetary and Space Science*, *51*(4–5), 339–352. https://doi.org/10.1016/S0032-0633(02)00207-6

Lee, C. O., Jakosky, B. M., Luhmann, J. G., Brain, D. A., Mays, M. L., Hassler, D. M., et al. (2018). Observations and impacts of the 10 September 2017 solar events at Mars: An overview and synthesis of the initial results. *Geophysical Research Letters*, *45*(17), 8871–8885. https://doi.org/10.1029/2018GL079162

Lin, R. P. (1968). Observations of lunar shadowing of energetic particles. *Journal of Geophysical Research*, *73*(9), 3066–3071. https://doi.org/10.1029/JA073i009p03066

Lin, R. P. (1987). Solar particle acceleration and propagation. *Reviews of Geophysics*, *25*(3), 676. https://doi.org/10.1029/RG025i003p00676

Lin, R. P., Anderson, K. A., Ashford, S., Carlson, C., Curtis, D., Ergun, R., et al. (1995). A three-dimensional plasma and energetic particle investigation for the Wind spacecraft. *Space Science Reviews*, *71*(1–4), 125–153. https://doi.org/10.1007/BF00751328

Liuzzo, L., Poppe, A. R., Addison, P., Simon, S., Nénon, Q., & Paranicas, C. (2022). Energetic magnetospheric particle fluxes onto Callisto's atmosphere. *Journal of Geophysical Research: Space Physics*, *127*(11), 1–30. https://doi.org/10.1029/2022JA030915

Liuzzo, L., Poppe, A. R., & Halekas, J. S. (2022). A statistical study of the Moon's magnetotail plasma environment. *Journal of Geophysical Research: Space Physics*, *127*(4), 1–23. https://doi.org/10.1029/2022JA030260

Liuzzo, L., Poppe, A. R., Halekas, J. S., Simon, S., & Cao, X. (2021). Investigating the Moon's interaction with the terrestrial magnetotail lobe plasma. *Geophysical Research Letters*, *48*(9), 1–11. https://doi.org/10.1029/2021GL093566

Liuzzo, L., Poppe, A. R., Paranicas, C., Nénon, Q., Fatemi, S., & Simon, S. (2020). Variability in the energetic electron bombardment of Ganymede. *Journal of Geophysical Research: Space Physics*, *125*(9), 1–35. https://doi.org/10.1029/2020JA028347

Liuzzo, L., Simon, S., & Regoli, L. (2019a). Energetic electron dynamics near Callisto. *Planetary and Space Science*, *179*, 104726. https://doi.org/10.1016/j.pss.2019.104726

Liuzzo, L., Simon, S., & Regoli, L. (2019b). Energetic ion dynamics near Callisto. *Planetary and Space Science*, *166*, 23–53. https://doi.org/10.1016/j.pss.2018.07.014

Lucey, P. G. (2000). Potential for prebiotic chemistry at the poles of the Moon. In R. B. Hoover (Ed.), *Instruments, methods, and missions for astrobiology III* (Vol. 4137, pp. 84–88). https://doi.org/10.1117/12.411612

McFadden, J. P., Carlson, C. W., Larson, D., Ludlam, M., Abiad, R., Elliott, B., et al. (2008). The THEMIS ESA plasma instrument and in-flight calibration. *Space Science Reviews*, *141*(1–4), 277–302. https://doi.org/10.1007/s11214-008-9440-2

Milan, S. E. (2004). A simple model of the flux content of the distant magnetotail. *Journal of Geophysical Research*, *109*(A7), A07210. https://doi.org/10.1029/2004JA010397

Ness, N. F., Scearce, C. S., & Cantarano, S. C. (1967). Probable observations of the geomagnetic tail at 10^3 Earth radii by Pioneer 7. *Journal of Geophysical Research*, *72*(15), 3769–3776. https://doi.org/10.1029/JZ072i015p03769

Paulikas, G. A. (1974). Tracing of high-latitude magnetic field lines by solar particles. *Reviews of Geophysics*, *12*(1), 117. https://doi.org/10.1029/RG012i001p00117

Plainaki, C., Paschalis, P., Grassi, D., Mavromichalaki, H., & Andriopoulou, M. (2016). Solar energetic particle interactions with the Venusian atmosphere. *Annales Geophysicae*, *34*(7), 595–608. https://doi.org/10.5194/angeo-34-595-2016

Poppe, A. R., Farrell, W. M., & Halekas, J. S. (2018). Formation timescales of amorphous rims on lunar grains derived from ARTEMIS observations. *Journal of Geophysical Research: Planets*, *123*(1), 37–46. https://doi.org/10.1002/2017JE005426

Poppe, A. R., Fatemi, S., & Khurana, K. K. (2018). Thermal and energetic ion dynamics in Ganymede's magnetosphere. *Journal of Geophysical Research: Space Physics*, *123*(6), 4614–4637. https://doi.org/10.1029/2018JA025312

Poppe, A. R., Fillingim, M. O., Halekas, J. S., Raeder, J., & Angelopoulos, V. (2016). ARTEMIS observations of terrestrial ionospheric molecular ion outflow at the Moon. *Geophysical Research Letters*, *43*(13), 6749–6758. https://doi.org/10.1002/2016GL069715

Raeder, J., Cramer, W. D., Germaschewski, K., & Jensen, J. (2017). Using OpenGGCM to compute and separate magnetosphere magnetic perturbations measured on board low Earth orbiting satellites. *Space Science Reviews*, *206*(1–4), 601–620. https://doi.org/10.1007/s11214-016-0304-x

Reames, D. V. (1999). Particle acceleration at the Sun and in the heliosphere. *Space Science Reviews*, *90*(3/4), 413–491. https://doi.org/10.1023/A:1005105831781

Reames, D. V. (2013). The two sources of solar energetic particles. *Space Science Reviews*, *175*(1–4), 53–92. https://doi.org/10.1007/s11214-013-9958-9

Richardson, I. G., & Cane, H. V. (2010). Near-Earth interplanetary coronal mass ejections during solar cycle 23 (1996 - 2009): Catalog and summary of properties. *Solar Physics*, *264*(1), 189–237. https://doi.org/10.1007/s11207-010-9568-6

Størmer, C. (1955). *The polar aurora*. Clarendon Press.

Van Allen, J. A. (1970). Energetic particle phenomena in the Earth's magnetospheric tail. In B. M. McCormac (Ed.), *Particles and fields in the magnetosphere* (pp. 111–121). D. Reidel Publishing Company. https://doi.org/10.1007/978-94-010-3284-1_12

Van Allen, J. A., & Ness, N. F. (1969). Particle shadowing by the Moon. *Journal of Geophysical Research*, *74*(1), 71–93. https://doi.org/10.1029/JA074i001p00071

Winglee, R. M., & Harnett, E. M. (2007). Radiation mitigation at the Moon by the terrestrial magnetosphere. *Geophysical Research Letters*, *34*(21), L21103. https://doi.org/10.1029/2007GL030507

Winslow, R. M., Lugaz, N., Philpott, L. C., Schwadron, N. A., Farrugia, C. J., Anderson, B. J., & Smith, C. W. (2015). Interplanetary coronal mass ejections from MESSENGER orbital observations at Mercury. *Journal of Geophysical Research: Space Physics*, *120*(8), 6101–6118. https://doi.org/10.1002/2015JA021200

Xapsos, M. A., Stauffer, C., Jordan, T., Barth, J. L., & Mewaldt, R. A. (2007). Model for cumulative solar heavy ion energy and linear energy transfer spectra. *IEEE Transactions on Nuclear Science*, *54*(6), 1985–1989. https://doi.org/10.1109/TNS.2007.910850

Xu, X., Angelopoulos, V., Wang, Y., Zuo, P., Wong, H.-C., & Cui, J. (2017). The energetic particle environment of the lunar nearside: SEP influence. *The Astrophysical Journal*, *849*(2), 151. https://doi.org/10.3847/1538-4357/aa9186

Xu, Z., Guo, J., Wimmer-Schweingruber, R. F., Freiherr von Forstner, J. L., Wang, Y., Dresing, N., et al. (2020). First solar energetic particles measured on the lunar far-side. *The Astrophysical Journal Letters*, *902*(2), L30. https://doi.org/10.3847/2041-8213/abbccc

Zeitlin, C., Hassler, D. M., Guo, J., Ehresmann, B., Wimmer-Schweingruber, R. F., Rafkin, S. C. R., et al. (2018). Analysis of the radiation hazard observed by RAD on the surface of Mars during the September 2017 solar particle event. *Geophysical Research Letters*, *45*(12), 5845–5851. https://doi.org/10.1029/2018GL077760